2012

Oral exposure to methylmercury modifies the prostatic microenvironment in adult rats

INTERNATIONAL JOURNAL OF EXPERIMENTAL PATHOLOGY, HOBOKEN, v. 93, n. 5, p. 354-360, OCT, 2012
http://www.producao.usp.br/handle/BDPI/42801

INTERNATIONAL JOURNAL OF Experimental Pathology

Int. J. Exp. Path. (2012), 93, 354–360

ORIGINAL ARTICLE

Oral exposure to methylmercury modifies the prostatic microenvironment in adult rats

Daniela A. Fossato da Silva*, Fernando Barbosa Jr† and Wellerson R. Scarano*

**Department of Morphology, Institute of Biosciences, Univ Estadual Paulista, Botucatu, SP, Brazil and †Department of Clinical, Faculty of Pharmaceutical Sciences, Toxicological and Bromatological Analysis, University of São Paulo, Ribeirão Preto, SP, Brazil*

INTERNATIONAL JOURNAL OF EXPERIMENTAL PATHOLOGY

doi: 10.1111/j.1365-2613.2012.00825.x

Received for publication: 18 November 2011
Accepted for publication: 7 May 2012

Correspondence:
Daniela Alessandra Fossato da Silva
Department of Morphology, Institute of Biosciences
UNESP, Univ Estadual Paulista
Distrito de Rubião Jr s/n
Botucatu
São Paulo, Brazil
CEP 18618-000
Tele/Fax: +55 14 3811 6264
E-mail: dani_fossato@yahoo.com.br

SUMMARY

Methylmercury (MeHg) is an environmental pollutant that is highly toxic to the central nervous system. As its effects on male reproductive system are poorly understood, this study was carried out to analyse the effects of MeHg on the rat prostate. To evaluate the MeHg toxicity on ventral prostate, three groups of adult male Wistar rats received oral doses of 0.5, 1.0 and 3.0 mg/kg MeHg, respectively, on a daily basis for 14 days. A fourth group was used as a control. The prostate weight was decreased in rats treated orally with 0.5 mg/kg MeHg compared to controls. Also, Hg concentration increased significantly in the prostate after treatments. There were reductions in serum testosterone levels and androgen receptor immunoreactivity in animals receiving 3.0 mg MeHg/kg. The stereological data showed changes in the prostatic epithelial, stromal and luminal compartments which varied according to the different doses. Histopathological alterations, such as chronic inflammation, stratified epithelial hyperplasia and epithelial inflammatory reactive atypia, were observed in the 0.5 mg/kg MeHg-treated group. Epithelial atrophy was observed in the 3.0 mg/kg MeHg-treated group. In conclusion, the MeHg affects prostatic homoeostasis resulting in histopathological changes that may be relevant in the pathogenesis of prostatic disease.

Keywords
adult male rat, androgen receptor, index proliferation, methylmercury, reproductive toxicity, ventral prostate

Mercury is a widespread environmental contaminant that enters the environment from a variety of industrial processes as well as from the earth's crust (Nriagu 1979). Mercury (Hg) is converted into methylmercury (MeHg) by aquatic bacteria and is passed along the food chain where it accumulates in fish and marine mammals.

Serious poisoning episodes, including those in Minamata (Japan) and Iraq during the 1950s and 1970s, led to acute MeHg intoxication, manifesting as severe nervous system disturbances in thousands of local inhabitants (Franco *et al.* 2009).

MeHG is found mostly as a complex with free cysteine and with proteins and peptides containing that amino acid. The methylmercuric-cysteinyl complex is recognized by amino acid transporting proteins in the body as methionine, another essential amino acid (Kerper *et al.* 1992). Because of this mimicry, it is transported freely throughout the body including across the blood–brain barrier and across the placenta, where it is absorbed by the developing foetus. Also for this reason as well as its strong binding to proteins, MeHg is not readily eliminated. The MeHg toxic effects are probably mediated via interaction with many of the vital enzymes involved in antioxidant regulation (Branco *et al.* 2012).

MeHg poisoning can result in several pathological conditions, including microcephaly, mental retardation, cerebral palsy, seizures, ataxia, anaemia, behavioural disturbances and reproductive dysfunction (Myers & Davidson 1998).

Growing evidences have indicated that exposure to MeHg can decrease male fertility (Khera 1973; Rao 1989; Rao & Gangadharan 2008). MeHg can pass through the blood–testis barrier acting directly on developing germ cells to alter spermatogenesis (Lee & Dixon 1975; Homma-Takeda *et al.* 2001). In rats, daily injections of MeHg can decrease both testicular and epididymal weight leading to increased cellular atrophy (Burton & Meikle 1980; Sun & Lin 1992) and

germ cell apoptosis (Homma-Takeda *et al.* 2001). Previous studies have emphasized that the exposure to MeHg decrease testosterone levels (Vachhrajani & Chowdhry 1990; Vachhrajani *et al.* 1992; Homma-Takeda *et al.* 2001; McVey *et al.* 2008). In addition, our recent study showed that MeHg reduced serum testosterone levels in a dose-dependent manner (Fossato da Silva *et al.* 2011), indicating this metal as a potential endocrine disruptor (ED).

The prostate is an accessory gland, androgen dependent, of the male urogenital system that contributes to the production of seminal fluid components and promotes the maintenance of ionic gradient and appropriate pH (Untergasser *et al.* 2005). At present, there is considerable clinical-pathological interest in the prostate and its pathophysiology because prostate cancer is now the most frequently diagnosed cancer among men and the second leading cause of male cancer deaths in the United States (Potosky *et al.* 1995; Parker *et al.* 1996). Additionally, the pathogenesis of prostate cancer reflects both hereditary and environmental conditions.

In rodents several aspects of prostatic changes related to chronic inflammation have been investigated. It appears that chemical trauma, dietary factors, steroid hormones or combinations of different environmental factors are all involved (De Marzo *et al.* 2007). Therefore, environmental factors act as EDs that can contribute to the development of prostatic diseases.

As the prostate is involved in several pathophysiological processes and as its functions may be compromised during MgHg exposure because of hormonal disturbances, the aim of this study was to evaluate the effects of subacute exposure to different doses of MeHg on the rat ventral prostate, focusing on histopathological and immunohistochemical parameters.

Material and methods

Animals

Adult male Wistar rats (n = 60), 80 days of age, (300–350 g) were used for the study. Animals were obtained from Central Biotherium of the UNESP – Univ Estadual Paulista and housed in polypropylene cages (43 cm × 30 cm × 15 cm) with laboratory-grade pine shavings as bedding. Rats were maintained under controlled temperature (23 ± 1°C) and lighting conditions (12:12-h photoperiod). Balanced rat chow (Purina®) and filtered tap water were provided *ad libitum*. Animals were allowed to adapt for at least 1 week before the beginning of the experiment. The experimental protocol followed the Ethical Principles in Animal Research of the Brazil College of Animal Experimentation and was approved by the Institute of Biosciences/UNESP Ethics Committee for Animal Experimentation (Protocol n°: 05/08).

Experimental design

Rats were divided into four groups (n = 15): Control, 0.5, 1.0 or 3.0 mg/kg body weight/day MeHg orally (by gavage) administered during 14 consecutive days (Fossato da Silva *et al.* 2011). The doses used in our study are common in reproductive toxicity induced by MeHg (McVey *et al.* 2008) and in other experimental studies (Robinson *et al.* 2010; Tonk *et al.* 2010). MeHg commercial solution (1 g/l) was purchased from Merck® (Merck KGaA, Darmstadt, Germany), dissolved in methanol (CH_3OH) (Sigma Aldrich®, St. Louis, MO, USA) and Milli-Q water (Millipore®, Billerica, MA, USA). Control group received distilled water by gavage.

Ventral prostates of ten rats per group were collected, weighed and their fragments processed for histopathological and morphometric-stereological analysis, and both for androgen receptor (AR) expression and for expression of an antigen associated with cell proliferation, Ki67, by immunohistochemistry (IHC). Prostate fragments were removed from the other five rats per group to quantify Hg by ICP-MS (Fossato da Silva *et al.* 2011).

Body weight and organ weights

On the 14th day after the MeHg exposure, all rats were weighed and anaesthetized with CO_2 followed by decapitation. After decapitation, the ventral prostates were removed (n = 10/group) and their weights (absolute and relative) were determined.

Determination of Mercury (Hg) level

Prior to sample collection, plastic tips and bottles (Nalgen) used in the procedure were cleaned by soaking in 10% (v/v) nitric acid (HNO_3) for 24 h and rinsing five times in Milli-Q water, then dried in a class containing 100 laminar flow hood to avoid contamination. Analyses for Hg were carried out using a quadrupole inductively coupled plasma mass spectrometer (ICP-MS ELAN DRCII, PerkinElmer, SCIEX, Norwalk, CT, USA). The sample introduction system was composed of a quartz cyclonic spray chamber and a Meinhard® nebulizer connected by Tygon® tubes to the ICP-MS peristaltic pump (set at 20 rpm). Other instrumental settings and operative conditions are reported in Fossato da Silva *et al.* (2011).

Hg analysis in ventral prostate was carried out according to Batista *et al.* (2009) by weighing approximately 75 mg of each tissue into conical tubes (15 ml). Then 1 ml of 50% (v/v) tetramethylammonium hydroxide (TMAH) solution was added to the samples, which were incubated at room temperature for 12 h and the volume increased up to 10 ml with a solution containing 0.5% (v/v) HNO_3, 0.01% (v/v) Triton® X-100. Analytical calibration standards were prepared daily over the range of 0–20 μg/l in diluents containing 5% (v/v) TMAH, 0.5% (v/v) HNO_3 and 0.01% (v/v) Triton® X-100.

Quality control of the results

Quality control of prostate Hg levels was acquired by the analysis of Certified Reference Materials (CRMs) purchased from National Research Council Canada (NRCC) (DOLT-3,

DORM-3 and TORT-2). Recovery ratios of Hg in all CRMs were always in the range of 95–105%.

Histopathological analysis

The ventral prostate (n = 10/group) was removed, and fragments selected from the distal part were fixed by immersion in buffered formalin phosphate-buffered saline (PBS) for 24 h. Fixed tissue samples were dehydrated in a graded ethanol series and embedded in glycol methacrylate resin (Leica historesin embedding kit Image-ProPlus, Media Cybernetics, Nussloch, Germany). Histological sections (3 μm) were subjected to haematoxylin–eosin (H&E) staining for general studies. Histopathological and stereological analyses were carried out on Leica and Olympus photomicroscopes, and the microscopic fields were digitized using the software Image-Pro®Plus version 4.5 for Windows™ Bethesda, MD, USA.

Morphometric-stereological analysis

Resin embedded sections were stained by H&E and quantitated by means of an imaging analysis system (Image-Pro®Plus version 4.5 for Windows™ software). For this purpose 100 histological fields randomly chosen from the distal part of the ventral prostate were captured and analysed via the stereological method with all histological fragments equally evaluated (n = 20/animal). Stereological analyses were obtained by Weibel's multipurpose graticulate, with 120 points and 60 test lines (Weibel 1963) to compare the relative proportions among the prostatic components (epithelium, stroma and lumen) in the experimental groups.

Immunohistochemistry

Androgen receptor (AR) (1:100/SC-816, rabbit polyclonal IgG, epitope mapping at the N-terminus of AR; Santa Cruz Biotechnology, Santa Cruz, CA, USA) and Ki67 (1:100/ab16667; Ki67 – Proliferation Marker, abcam®, Cambridge, MA, USA) primary antibodies were used for IHC assay. The IHC reaction was performed using the avidin–biotin complex (ABC) kit (Santa Cruz Biotechnology) for AR and the Mach4™ BioCare Polymer kit (Biocare Medical, concord, CA, USA) for Ki67. For IHC, the ventral prostates were fixed in formaldehyde buffered PBS (10%), dehydrated in alcohol and embedded in paraplast. The sections (5 μm) were dewaxed and then rehydrated in graded alcohol and distilled water. Antigen retrieval was conducted in sodium citrate buffer (pH = 6.0) at high temperature (~100 °C) by steam cooker during 45–50 min. Endogenous peroxidase activity was blocked with 0.3% hydrogen peroxide in methanol for 30 min, followed by a quick rinse in distilled water and PBS and then incubated in 1% bovine serum in PBS for 1 h or Background Sniper (Biocare®) for 15 min, to block non-specific binding. Sections were incubated with the primary antibody at 4 °C overnight. The slides were then incubated with biotinylated secondary antibody at 37 °C followed by peroxidase-conjugated avidin–biotin complexes and chromogen diaminobenzidine (DAB) and HRP-Polymer (Biocare®). The sections were finally counterstained with Harris's haematoxylin. As a negative control, the primary antibody was replaced with the corresponding normal isotype serum.

AR semi-quantitative analysis

Five histological sections were analysed per group, and 10 AR-positive nuclei were randomly selected by section (50 nuclei/group). The images of the selected nuclei were cut in a regular and constant rectangular form (always in central part of the nucleus, in view of the homogeneity of nuclear staining/reactivity for AR) and those 'rectangles' were submitted to optical densitometry analyser using SCION Image for Windows Software® (Fossato da Silva *et al.* 2011).

Antigen for cell proliferation (Ki67)

The number of epithelial cells which express Ki67 was counted in 50 fields/group, at 400× magnification from five different prostate fragments (10 fields/each fragment) and expressed as percentage of the total cells counted. All image acquisition and quantitative measurements were carried out in a blinded fashion to both animal identity and experimental condition.

Statistical analysis

All results from the MeHg-treated groups *vs.* control group were statistically compared by the non-parametric Kruskal–Wallis test, complemented by the Dunns test in the GraphPad Prism® software. Values are expressed as mean ± SEM and medians (Q_1–Q_3). Statistical significance was set at $P < 0.05$.

Results

The absolute and relative weight of the ventral prostate was seen to decrease after 0.5 mg/kg MeHg administration compared to control group (Table 1). The level of Hg increased significantly in the prostate of all treated groups, showing a direct relationship between the administered dose and Hg concentration in the tissue. Accordingly, the 3.0 mg/kg MeHg-treated animals contained higher levels of prostatic Hg than the other groups (Table 1). The body weight did not differ among the groups (data not shown).

Inflammatory foci were observed in 60% of the animals treated with 0.5 mg/kg MeHg and consisted mainly of mononuclear cells (predominantly small lymphocytes) with an increase in blood vessels in the stroma (Figure 1c), as well as stratified focal hyperplasia (Figure 1d).

In the 1.0 mg/kg MeHg-treated group, the appearance of periacinar connective tissue was identified adjacent to the epithelium, causing epithelial folds (Figures 1e–f). In 3.0 mg/kg MeHg group, the glandular epithelium presented a predominantly low cubic and squamous aspect (Figures 1g–h). The

Table 1 Absolute and relative prostate weight and prostate mercury levels in control group and methylmercury (MeHg)-treated groups at doses 0.5, 1.0 and 3.0 mg/kg after 14 days of MeHg treatment

Parameters	Control (n = 9)	0.5 mg/kg (n = 10)	1.0 mg/kg (n = 10)	3.0 mg/kg (n = 10)
Prostate (mg)	510.79 ± 22.41	421.54 ± 19.54*	523.85 ± 14.83	486. 65 ± 29.51
Prostate (mg/100 g)	126.25 ± 7.76	103.73 ± 4.15*	120.68 ± 3.91	126.90 ± 6.04
Mercury (μg/ml)	0.01 ± 0.01	0.29 ± 0.02	0.71 ± 0.04	2.06 ± 0.03**

Values are expressed as mean ± SEM.
*$P < 0.05$.
**$P < 0.01$.
Non-parametric Kruskall–Wallis test, complemented by Dunns test.

nuclear-to-cytoplasmic ratio was apparently higher in these animals than in others. The changes in the epithelium and the accumulation of secretion in the lumen could have contributed to the dilation of glandular acini, increasing the glandular lumen in this experimental group (Figure 1g; Table 2).

Stereological data showed an increased epithelial component in the 0.5 and 1.0 mg/kg MeHg-treated groups, while the 3.0 mg/kg MeHg and control groups were unchanged. The stromal component decreased in the 1.0 and 3.0 mg/kg MeHg groups in relation to the control and 0.5 mg/kg MeHg groups. Also, the luminal component was increased after 3.0 mg/kg MeHg compared to other groups (Table 2).

AR immunoreactivity was similar between control, 0.5 and 1.0 mg/kg MeHg groups (Figure 2a–c, e). However, after 3.0 mg/kg MeHg, the AR labelling showed lower intensity in the epithelial cells (Figure 2d–e). The proliferation index (as judged by numbers of Ki67-positive cells showed a significant increase after treatment only in the 0.5 mg/kg MeHg group compared to control and other groups (control: median = 0.55%; 0.5 mg/kg MeHg: median = 1.35%*; 1.0 mg/kg MeHg: median = 0.6%; 3.0 mg/kg MeHg: median = 0.5%; *$P \leq 0.05$).

Discussion

Although several studies have reported the toxicity of MeHg in some bodily systems, such as nervous system (Sanfeliu *et al.* 2003; Crespo-López *et al.* 2005) and immune system (Häggqvist *et al.* 2005), there are few reports about the

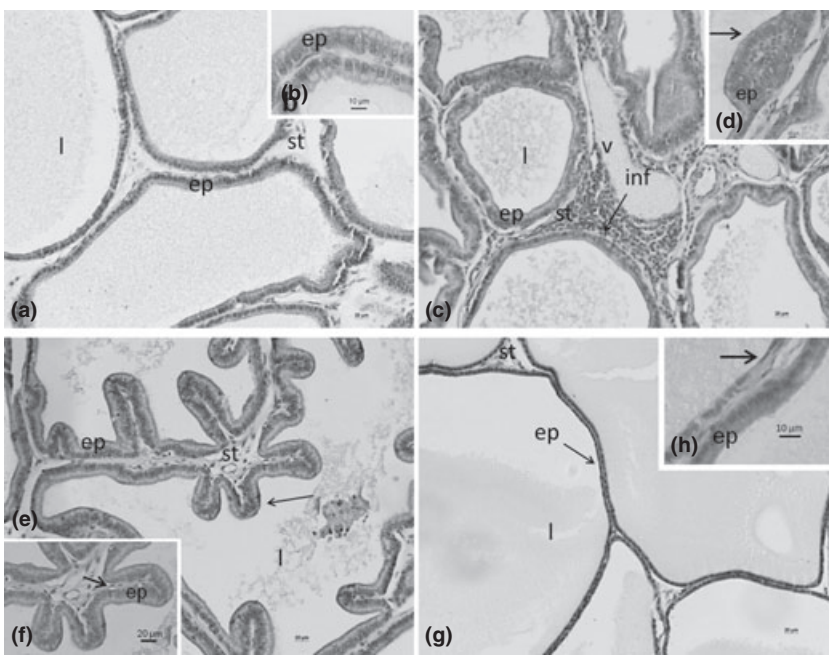

Figure 1 Haematoxylin–eosin (H&E) staining. (a–b) Histological sections from Control Group ventral prostate; a: general aspect of the distal segment of the gland; b: detail of the epithelium. (c–d) Histological sections from 0.5 mg/kg methylmercury (MeHg)-treated group; c, general aspect of the distal segment of the gland. Inflammatory focus (inf/arrow) occupying the stroma (st) of the gland; presence of large veins (v); d, detail showing an epithelial hyperplasia (arrow). (e–f) Histological sections from 1.0 mg/kg MeHg-treated group: e, general aspect of the gland showing papillary hyperplasia with folds (arrow) in the supporting vascularized connective tissue; (f) detail of the epithelial fold. The arrow indicates the connective tissue inserted in an epithelial fold. (g–h) Histological sections from 3.0 mg/kg MeHg-treated group: g: prostatic acini at low magnification. There is evidence of an increase in the luminal compartment; h, Detail showing the squamous dysplasia of epithelium. The arrow points to the flattened cells. General abbreviations: epithelium (ep); stroma (st); lumen (lu); inflammatory focus (inf); blood vessel (v).

Table 2 Weibel's stereology analyses of control group and methylmercury (MeHg)-treated groups at doses of 0.5, 1.0 and 3.0 mg/kg after 14 days of MeHg treatment; $n = 50$ fields/group

Relative Proportion (%)	Control	0.5 mg/kg	1.0 mg/kg	3.0 mg/kg
Epithelium	19.94 (17.26–23.95)	27.97 (23.51–33.48)***	26.78 (23.36–32.14)***	16.07 (11.90–21.42)
Stroma	18.75 (11.45–23.95)	16.37 (12.94–25.14)	10.12 (8.18–17.70)*	8.33 (5.95–11–45)***
Lumen	59.82(51.48–66.07)	54.76 (44.49–59.67)	62.50 (49.85–66.96)	75.00 (66.96–79.46)***

Values are expressed as median (Q1–Q3).
*$P < 0.05$.
***$P < 0.001$.
Non-parametric Kruskall–Wallis test, complemented by Dunns test.

MeHg effects on the male reproductive system (Homma-Takeda *et al.* 2001; Fossato da Silva *et al.* 2011). Fossato da Silva *et al.* (2011) using the same experimental protocol showed that testosterone levels decrease after a dose of 3.0 mg/kg MeHg. Therefore, previous results obtained by Fossato da Silva and collaborators (Fossato da Silva *et al.* 2011) will be considered for the discussion.

It is known that environmental and dietary factors are probably responsible for causing significant changes in the concentrations and metabolism of sex steroid hormones, which contribute to the development of prostatic lesions and diseases (Hsing & Devesa 2001) as they epidemiologically manifest in regions of high exposure to EDs.

The prostate weight decreased after 0.5 mg/kg MeHg and this seems to be associated with a local effect of MeHg, since other markers, such as systemic hormone levels and body weight were not altered in this group. Another hypothesis could be that the accumulation of MeHg, which in low doses can act as an anti-androgenic agent by blocking enzymes, such as aromatase, which converts testosterone into dihydrotestosterone.

The increase in MeHg in the tissue may be related to increased oxidative stress (Crespo-López *et al.* 2009) and consequently to the adaptive rearrangement of the gland because of local stress. Increases in the epithelial compartment of the 0.5 mg/kg MeHg group reflect the prostatic

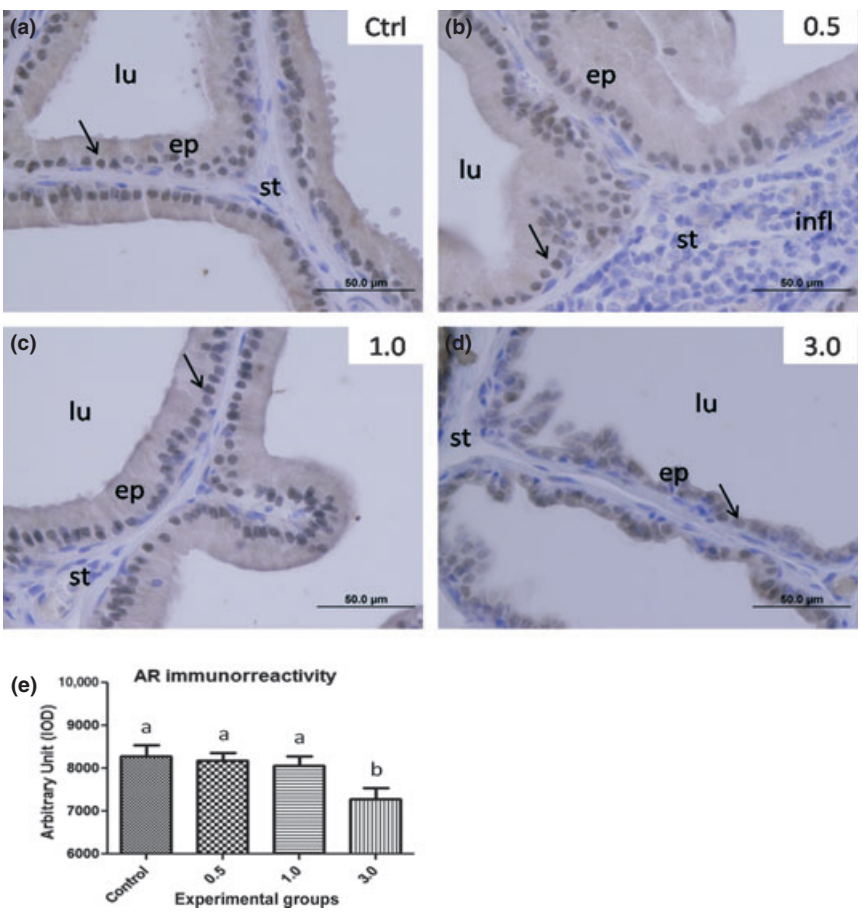

Figure 2 Histological sections submitted to androgen receptor (AR) immunohistochemistry. (a) Control Group; (b) (0.5 mg/kg methylmercury (MeHg)-treated group); (c) (1.0 mg/kg MeHg-treated group); (d) (3.0 mg/kg MeHg-treated group): note that there is marked epithelial atrophy with more compact nuclei and a great reduction in cytoplasmic volume. Brown stain signifies AR-positive reactivity. The arrows indicate AR-positive cells. General abbreviations: epithelium (ep); stroma (st); lumen (lu); inflammatory focus (inf). (e) Semi-quantitative analysis (IOD integrated optical density) of the nuclear epithelial cells ($n = 50$ nuclei/group) AR immunoreactivity from prostate following MeHg treatment at doses of 0.5, 1.0 and 3.0 mg/kg for 14 days. Values are expressed as means ± SEM. Different 'letters' indicate significant difference among the groups ($P \leq 0.05$).

tissue adaptation to Hg accumulation (Crespo-López *et al.* 2009). A third aspect to be considered is the reactive induction produced by stromal inflammatory cells as small lymphocytes associated with epithelial proliferation (Shappell *et al.* 2004).

In the 1.0 mg/kg MeHg-treated group, an increase in the epithelial and a decrease in the stromal compartments were observed. These features may be associated with the disruption produced by mercury in the tissue and by the decrease in the testosterone availability. This aspect could be important in trying to justify the folding of the epithelial layer and the appearance of adjacent connective tissue, which can be observed in the experiments followed by castration (Vilamaior *et al.* 2000; Scarano *et al.* 2008).

A significant increase in the luminal component and a reduction in other components were observed in the 3.0 mg/kg MeHg group. These modifications are supported by epithelial atrophy and dilation of the glandular acini, which seems to be primarily because of a decrease in testosterone levels (Crespo-López *et al.* 2009). Furthermore, it is well-known that MeHg adversely alters male steroidogenesis, (Vachhrajani & Chowdhry 1990; McVey *et al.* 2008). Results from chemical and surgical castration using experimental models revealed similar glandular atrophy in the prostate (Vilamaior *et al.* 2000; Oliveira *et al.* 2007; Scarano *et al.* 2008).

Tissue changes such as reactive epithelial atypia and stratified hyperplasia have been observed in the 0.5 MeHg-treated group, which presented frequent chronic inflammation. The same histopathological feature was found in a study using low doses of di-n-butyl-phthalate (DBP) during pregnancy and lactation (Scarano *et al.* 2009) and after xenoestrogen treatments such as diethylstilbestrol (Timms *et al.* 2005). In rodents, the aspects which could be related to the chronic inflammation include chemical trauma, dietary factors, steroid hormones or combinations of different environmental factors (De Marzo *et al.* 2007). It is important because epidemiological, histopathological and molecular pathological studies in humans have also demonstrated evidence that inflammation is involved in the pathogenesis of prostate cancer (De Marzo *et al.* 2004, 2007; Palapattu *et al.* 2005).

Our results demonstrate that for each MeHg treatment, there has been an association with a typical histopathological response pattern. Moreover MeHg interfered with the homoeostasis of the gland; however, in the 0.5 mg/kg MeHg treatment, there was a compensatory effect. Conversely, in the 3.0 mg/kg MeHg treatment group, there was a decrease in glandular activity, probably due to the endocrine imbalance caused by the decrease in testosterone. The lowest dose was seen to cause a slight imbalance that was reflected by an adaptive response, creating focal changes such as an inflammatory response and an increase in epithelial cell volume and proliferation. Curiously, this pattern of biological response has been reported in studies using anti-androgens such as Vinclozolin (Cowin *et al.* 2008), di-n-butyl-phthalate (Scarano *et al.* 2009), and after oestrogen diethylstilbestrol (DES) treatments (Timms *et al.* 2005). High doses of DES during pregnancy may inhibit the development of prostatic ducts; however, low doses can stimulate the proliferation and prostate development, as already evidenced in foetuses exposed to DES (Timms *et al.* 2005).

Part of the changes may be related to AR inactivation caused by intracellular signalling proteins or by the bioavailability of ligands (hormone or antagonist) (Feldman & Feldman 2001). The presence of inflammatory cells was related to a dose of 0.5 mg/kg MeHg group. Paracrine signals mediated by inflammatory factors can influence the differentiation and adaptation of epithelial and stromal cells, leading to dysplasia of the gland, reactive epithelial atypia and stromal remodelling (Cowin *et al.* 2008; Scarano *et al.* 2009).

No changes were observed in the semi-quantitative pattern of AR immunoreactivity in 0.5 and 1.0 MeHg-treated groups as compared to the control group. However, there was a reduction of AR immunoreactivity in the 3.0 MeHg-treated group. This fact may be related to the reduced bioavailability of the agonist (testosterone) and suggests a reduction of AR activation and migration to nucleus, decreasing the glandular activity, which could be directly related to epithelial atrophy (Feldman & Feldman 2001).

The histopathology of the ventral prostate demonstrated different responses pattern according to the MeHg dosage. Also, there were tissue alterations in all treatments, suggesting that MeHg, directly or indirectly, affects the prostatic microenvironment homoeostasis.

Acknowledgements

This study was supported by the Fundação de Amparo à Pesquisa do Estado de São Paulo (FAPESP, Grant 2007/56458-4). The authors are grateful to José Eduardo Bozano for technical assistance and to Dr. Sebastião Roberto Taboga (Department of Biology, IBILCE, UNESP, São José do Rio Preto, SP, Brazil) for their assistance with the photographic registration.

Conflict of interest

The authors declare that they have no conflict of interest.

References

Batista B.L., Grotto D., Rodrigues J.L., Souza V.C.O., Barbosa F. Jr (2009) Determination of trace elements in biological samples by inductively coupled plasma mass spectrometry with tetramethylammonium hydroxide solubilization at room temperature. *Anal. Chim. Acta* **646**, 23–29.

Branco V., Canário J., Lu J., Holmgren A., Carvalho C. (2012) Mercury and selenium interaction in vivo: effects on thioredoxin reductase and glutathione peroxidase. *Free Radic. Biol. Med.* **52**, 781–793.

Burton G.V. & Meikle A.W. (1980) Acute and chronic methyl mercury poisoning impairs rat adrenal and testicular function. *J. Toxicol. Environ. Health* **6**, 597–606.

Cowin P.A., Foster P., Pedersen J., Hedwards S., McPherson S.J., Risbridger G.P. (2008) Early-onset endocrine disruptor-induced prostatitis in the rat. *Environ. Health Perspect.* **116**, 923–929.

Crespo-López M.E., Herculano A.M., Corvelo T.C., Do Nascimento J.L.M. (2005) Mercury and neurotoxicity. *Rev. Neurol.* **40**, 441–447.

Crespo-López M.E., Macêdo G.L., Pereira S.I. *et al.* (2009) Mercury and human genotoxicity: critical considerations and possible molecular mechanisms. *Pharmacol. Res.* **60**, 212–220.

De Marzo A.M., De Weese T.L., Platz E.A. *et al.* (2004) Pathological and molecular mechanisms of prostate carcinogenesis: implications for diagnosis, detection, prevention, and treatment. *J. Cell. Biochem.* **91**, 459–477.

De Marzo A.M., Platz E.A., Sutcliffe S. *et al.* (2007) Inflammation in prostate carcinogenesis. *Nat. Rev. Cancer* **7**, 256–269.

Feldman B.J. & Feldman D. (2001) The development of androgen-independent prostate cancer. *Nature* **1**, 34–45.

Fossato da Silva D.A., Teixeira C.T., Scarano W.R. *et al.* (2011) Effects of methylmercury on male reproductive functions in Wistar rats. *Reprod. Toxicol.* **31**, 431–439.

Franco J.L., Posser T., Dunkley P.R. *et al.* (2009) Methylmercury neurotoxicity is associated with inhibition of the antioxidant enzyme glutathione peroxidase. *Free Radic. Biol. Med.* **47**, 449–457.

Häggqvist B., Havarinasab S., Björn E., Hultman P. (2005) The immunosuppressive effect of methylmercury does not preclude development of autoimmunity in genetically susceptible mice. *Toxicology* **208**, 149–164.

Homma-Takeda S., Kugenuma Y., Iwamuro T., Kumagai Y., Shimojo N. (2001) Impairment of spermatogenesis in rats by methylmercury: involvement of stage- and cell- specific germ cell apoptosis. *Toxicology* **169**, 25–35.

Hsing A.W. & Devesa S.S. (2001) Trends and patterns of prostate cancer: what do they suggest? *Epidemol. Res.* **23**, 3–13.

Kerper L.E., Ballatori N., Clarkson T.W. (1992) Methylmercury transport across the blood-brain barrier by an amino acid carrier. *Am. J. Physiol.* **262**, R761–R765.

Khera K.S. (1973) Reproductive capability of male rats and mice treated with methyl mercury. *Toxicol. Appl. Pharmacol.* **24**, 167–177.

Lee I.P. & Dixon L. (1975) Effects of mercury on spermatogenesis studied by velocity sedimentation cell separation and serial mating. *J. Pharmacol. Exp. Ther.* **193**, 171–181.

McVey M.J., Cooke G.M., Curran I.H.A. *et al.* (2008) An investigation of the effects of methylmercury in rats fed different dietary fats and proteins: testicular steroidogenic enzymes and serum testosterone levels. *Food Chem. Toxicol.* **46**, 270–279.

Myers G.J. & Davidson P.W. (1998) Prenatal methylmercury exposure and children: neurologic, developmental and behavioral research. *Environ. Health. Perpect.* **106**, 841–847.

Nriagu J.O. (1979) Global inventory of natural and anthropogenic emissions of trace metals to the atmosphere. *Nature* **279**, 409–411.

Oliveira S.M., Leite Vilamaior P.S., Corradi L.S., Góes R.M., Taboga S.R. (2007) Cellular and extracellular behavior in the gerbil (Meriones unguiculatus) ventral prostate following different types of castration and the consequences of testosterone replacement. *Cell Biol. Int.* **31**, 235–245.

Palapattu G.S., Sutcliffe S., Bastian P.J. *et al.* (2005) Prostate carcinogenesis and inflammation: emerging insights. *Carcinogenesis* **26**, 1170–1181.

Parker S.L., Tong T., Bolden S., Wingo P.A. (1996) Cancer statistics. *CA Cancer J. Clin.* **65**, 5–27.

Potosky A.L., Miller B.A., Albertsen P.C., Kramer B.S. (1995) The role of increasing detection in the rising incidence of prostate cancer. *JAMA* **273**, 548–552.

Rao M.V. (1989) Histophysiological changes of sex organs in methylmercury intoxicated mice. *Endocrinol. Exp.* **23**, 55–62.

Rao M.V. & Gangadharan B. (2008) Antioxidative potential of melatonin against mercury induced intoxication in spermatozoa in vitro. *Toxicol. In Vitro* **22**, 935–942.

Robinson J.F., Griffith W.C., Yu X., Hong S., Kim E., Faustman E.M. (2010) Methylmercury induced toxicogenomic response in C57 and SWV mouse embryos undergoing neural tube closure. *Reprod. Toxicol.* **30**, 284–291.

Sanfeliu C., Sebastia J., Cristofol R., Rodriguez-Farre E. (2003) Neurotoxicity of organomercurial compounds. *Neurotox. Res.* **5**, 283–305.

Scarano W.R., de Sousa D.E., Campos S.G., Corradi L.S., Vilamaior P.S., Taboga S.R. (2008) Oestrogen supplementation following castration promotes stromal remodelling and histopathological alterations in the Mongolian gerbil ventral prostate. *Int. J. Exp. Pathol.* **89**, 25–37.

Scarano W.R., Toledo F.C., Guerra M.T. *et al.* (2009) Long-term effects of developmental exposure to di-n-butyl-phthalate (DBP) on rat prostate: proliferative and inflammatory disorders and a possible role of androgens. *Toxicology* **262**, 215–223.

Shappell S.B., Thomas G.V., Roberts R.L. *et al.* (2004) Prostate pathology of genetically engineered mice: definitions and classification. The consensus report from the Bar Harbor Meeting of the mouse models of human cancer consortium prostate pathology committee. *Cancer Res.* **64**, 2270–2305.

Sun Z.W. & Lin X.W. (1992) The effect of methylmercury on testicular function of mice. *Zhonghua Yu Fang Yi Xue Za Zhi.* **26**, 159–161.

Timms B.G., Howdeshell K.L., Barton L., Bradley S., Richter C.A., vom Saal F.S. (2005) Estrogenic chemicals in plastic and oral contraceptives disrupt development of the fetal mouse prostate and urethra. *Proc. Natl Acad. Sci. USA* **102**, 7014–7019.

Tonk E.C.M., Groot D.M.G., Penninks A.H. *et al.* (2010) Developmental Immunotoxicity of Methylmercury: The Relative Sensitivity of Developmental and Immune Parameters. *Toxicol. Sci.* **117**, 325–335.

Untergasser G., Madersbacher S., Berger P. (2005) Benign prostatic hyperplasia: age-related tissue-remodeling. *Exp. Gerontol.* **40**, 121–128.

Vachhrajani K.D., Chowdhry A.R. (1990) Distribution of mercury and evaluation of testicular steroidogenesis in mercuric chloride and methylmercury administered rats. *Indian J. Exp. Biol.* **28**, 746–751.

Vachhrajani K.D., Chowdhury A.R., Dutta K.K. (1992) Testicular toxicity of methylmercury: analysis of cellular distribution pattern at different stages of the seminiferous epithelium. *Reprod. Toxicol.* **6**, 355–361.

Vilamaior P.S., Felisbino S.L., Taboga S.R., Carvalho H.F. (2000) Collagen fiber reorganization in the rat ventral prostate following androgen deprivation: a possible role for smooth muscle cells. *Prostate* **45**, 253–258.

Weibel E.R. (1963) Principles and methods for the morphometric study of the lung and other organs. *Lab. Invest.* **12**, 131–155.